Williamsburg, Virginia
ACTIVE 04
2004 September 20-22

Improved Inlet Noise Attenuation by Alteration of Boundary Layer Profiles

Ramani Mani, NRC Research Associate, NASA Langley Research Center, MS 463, 2 North Dryden Street, Hampton, VA 23681-2199, USA, r.mani@larc.nasa.gov
Jon Luedke, GE Global Research, ES 220A, One Research Circle, Niskayuna, NY 12309, USA, luedke@crd.ge.com
Michael G. Jones, Douglas M. Nark, NASA Langley Research Center, MS 463, 2 North Dryden Street, Hampton, VA 23681-2199, USA, Michael.G.Jones@nasa.gov, Douglas.M.Nark@nasa.gov

ABSTRACT

Acoustic liners are an essential component of technology used to reduce aircraft engine noise. Flow affects attenuation due to the liner in several ways, one of which is that boundary layers adjacent to the liner refract the sound. In the case of inlet noise, the boundary layer causes sound to be refracted away from the liner, thus degrading attenuation. A concept to *improve attenuation by the liner by alteration of inlet boundary layer profiles* is presented. The alteration of profiles is achieved by inlet blowing. Computational fluid dynamics and duct mode propagation theory for ducts carrying a parallel sheared flow have been used to design experiments to explore such a possibility in the NASA Langley Research Center Grazing Incidence Tube using an inlet blowing scheme developed at General Electric Global Research. The effects of inlet blowing on two liner configurations were evaluated. Calculated results will be shown for blowing ratios (injected flow/duct flow) of approximately 12% and frequencies up to 3 kHz. These results emphasize changes of attenuation achieved by blowing for the two liners. Experimental results of measured flow profiles (with and without blowing) in the Grazing Incidence Tube, and of corresponding changes in attenuation by the liner due to blowing will be presented.

1. INTRODUCTION

It is well known that effects of flow on sound propagation in ducts are comprised of *both* convective effects and refractive effects. If there were only uniform convection (an idealization referred to as "plug" flow), flow effects on propagation would be restricted to wavelength lengthening (in the exhaust) or shortening (in the inlet) with no refraction. For the inlet case, convection increases the residence time of an acoustic energy packet over an absorbing surface, with the consequence of making the liner look acoustically longer. This *enhances* attenuation. The addition of refraction due to a boundary layer then complicates the purely convective effect. In the inlet, where sound propagates against the flow, boundary layers refract sound *away* from the inlet liner and thereby reduce the attenuation. The two effects are not linearly additive, but are instead *interactive* for inlet noise. For this case, contraction of the effective acoustic wavelength due to convection causes flow gradients to be considerably more effective in causing an alteration of wave fronts. This is contrasted with exhaust noise, where effective wavelengths are increased and flow gradients are less consequential. The effects are somewhat simple to understand in the case where the frequency – duct transverse dimension combination is such that only the lowest mode of acoustic propagation is sustained (in the hard wall portion of the duct). The current paper is limited to studies where this situation would prevail in the NASA Langley Research Center Grazing Incidence Tube (GIT), with source excitation restricted to a maximum of 3 kHz. Only cases of inlet propagation (i.e., where sound propagates in a direction opposite to the mean flow) are considered. The reduction of attenuation by the liner due to refraction in the inlet case has already been noted. One way to not only mitigate this loss of attenuation but actually to enhance the attenuation would be to use *boundary layer blowing* (in the same direction as the main stream) such that the effective speed of sound near the walls is *lower* than that in the mid stream (unlike the case of conventional boundary layers) such that the inlet propagating sound is "turned into" the wall by refraction.

We report herein on an evaluation of this concept based on results achieved in the NASA Langley GIT. The paper is presented in the following sequence:

- A brief outline of relevant aspects of the theory of acoustic propagation of duct modes in the presence of flow gradients

- Use of CFD (computational fluid dynamics) to design and evaluate the effectiveness of blowing schemes to achieve desired boundary layer profiles, with a description of the required interfacing between the CFD and acoustic solutions
- Flow and acoustic measurements conducted in the NASA Langley Research Center GIT
- Summary

2. THEORETICAL EVALUATION OF EFFECTS OF BOUNDARY LAYER PROFILE CHANGE ON ATTENUATION BY A LINER

Solution Technique – Sound propagation in a two-dimensional duct carrying a parallel, sheared flow

The acoustic evaluation is carried out by examination of a simplified problem of discrete frequency sound propagation in a two dimensional duct carrying a parallel, sheared flow (figure 1). Thus, acoustic attenuations resulting from this analysis apply strictly to an infinitely lined duct with no variation of flow in the axial direction and with no account taken of transition from hardwall to soft wall. Linear, inviscid sound propagation is assumed, though the mean velocity profiles of the parallel, sheared flow are "realistic" in that the no-slip condition at the duct walls is satisfied. *All lengths are non-dimensionalized by the actual duct half-width*. Non-dimensional coordinates are indicated with underscored notation (e.g., as $\underline{x}$, $\underline{y}$). As shown in figure 1, the duct spans the region $\underline{y} = 0$ to $\underline{y} = 2$, and the positive $\underline{x}$-axis is in the downstream direction.

As in reference 1, assume solutions for the acoustic pressure (normalized by ρc^2, where ρ and c are the uniform air density and speed of sound in the duct) as $F(\underline{y})\exp[j(\omega t - khK\underline{x})]$, where $k = \omega/c$, $j = \sqrt{-1}$, h is the duct half width, and K is the non-dimensional axial propagation constant. As shown in reference 1, if $M(\underline{y})$ denotes the axial Mach number distribution in the duct as a function of $\underline{y}$ (primes denote differentiation with respect to $\underline{y}$), the acoustic pressure satisfies:

$$F'' + 2KM'F'/(1-MK) + \Omega^2((1-MK)^2 - K^2)F = 0 \text{ (where } \Omega = kh) \tag{1}$$

At $\underline{y} = 0$ (hard wall), $F' = 0$, and at the treated wall $\underline{y} = 2$, with A denoting the normalized admittance at the wall $\underline{y} = 2$ (oscillations in time are assumed to be of form $\exp(j\omega t)$ with $\omega > 0$):

$$F' = -j\Omega AF(1-MK)^2 \tag{2}$$

This system can also be written as (with $F_1 = F'/(1-MK)^2$):

$$F' = (1-MK)^2 F_1 \tag{3}$$

and

$$F_1' = -\Omega^2(1 - K^2/(1-MK)^2)F \tag{4}$$

The boundary conditions are $F_1 = 0$ at $\underline{y} = 0$ and $F_1 = -j\Omega AF$ at $\underline{y} = 2$. To solve an eigenvalue problem for the complex eigenvalue K in (1), the value of F at $\underline{y} = 0$ can be chosen as 1 without any loss of generality.

Analytic continuation is used to solve the $\underline{y}$-direction eigenvalue problem. First, consider a "plug" flow situation (duct carrying a uniform, or $\underline{y}$-independent, flow which is the average Mach number in the duct), with hard walls at both $\underline{y}$=0 and $\underline{y}$=2. In this case, the transverse mode functions can be written as $\cos(\beta\underline{y})$ where $\beta = n\pi/2$ and n = 0, 1, 2 …, etc. For a plug flow at Mach number M, the "dispersion relation" between β and axial (non-dimensional) wave number K is:

$$\beta^2 = \Omega^2((1-MK)^2 - K^2) \tag{5}$$

whose derivative (let $\beta' = d\beta/dK$) is:

$$\beta' = -\Omega^2(K(1-M^2) + M)/\beta \tag{6}$$

For the symmetric modes, the eigenvalue equation for a plug flow at Mach number M with admittance A would be:

$$\beta\sin(2\beta) = j\,\Omega\,A\cos(2\beta)\,(1-MK)^2 \tag{7}$$

By examining the differentials in this equation and using the expression for dβ/dK, we arrive at the following first order correction dK to a root K of the eigenvalue equation case as admittance is changed from A to A+dA. Let

$$f_1 = 2j\Omega MA(1-MK) - \Omega^2(K(1-M^2)+M)(T/\beta)(1+4\beta/\sin(4\beta)) \tag{8}$$

and

$$f_2 = j\Omega(1-MK)^2(dA) \tag{9}$$

where T is used to denote tan(2β). Then $dK = f_2 / f_1$.

For the first iteration (calculation) of dK starting from A = 0 and the case of the zeroth mode, certain limiting values are needed in this correction procedure as β approaches zero. However, this procedure yields only a first estimate of the correction. The actual root is found by Muller's method (reference 3). Other than this point of caution for the case of "starting" from A=0 and the zeroth root, the equation $dK = f_2 / f_1$ is applicable. It should also be noted that when starting from A=0 for non-zero modes, sin(2β) = 0 and cos(2β) is plus or minus unity. The limiting value of f_1 is then $-2\Omega^2(K(1-M^2)+M)$. Also, if β is known (for example for A=0 and symmetric cases as nπ/2), then K is given by:

$$K = -M/(1-M^2) \pm \Delta \text{ (upper sign for } \underline{x} > 0 \text{ and lower sign for } \underline{x} < 0) \tag{10}$$

where $\Delta^2 = 1/(1-M^2)^2 - \beta^2/((1-M^2)\,\Omega^2)$, $\Delta = \sqrt{\Delta^2}$ if $\Delta^2 > 0$ and $\Delta = \pm j\sqrt{-\Delta^2}$ if $\Delta^2 < 0$. If the starting (A=0) value of $\beta = n\pi/2$ exceeds $\Omega/(1-M^2)$ such that $\Delta^2 < 0$, then the hard wall mode for plug flow at M is "cut off".

In the antisymmetric cases, initial (A=0) values of β are (2n+1) π/4 for n-= 0,1,2, etc, and the initial mode functions are sin (β $\underline{y}$). The eigenvalue equation is:

$$\beta\cos(2\beta) = -j\,\Omega\,A\sin(2\beta)\,(1-MK)^2. \tag{11}$$

The root adjustment equation is now as follows. Let

$$f_1 = 2j\Omega MA(1-MK) + \Omega^2(K(1-M^2)+M)(Ct/\beta)(1-4\beta/\sin(4\beta)) \tag{12}$$

and

$$f_2 = j\Omega(1-MK)^2(dA) \tag{13}$$

where Ct denotes cot(2β). Then, $dK = f_2 / f_1$. Note that when starting from A=0, cos(2β) = 0 and sin(2β) is plus or minus unity. The limiting value of f_1 is again $-2\Omega^2(K(1-M^2)+M)$. Also, if β is known (e.g., for A=0 and antisymmetric cases as (2n+1)π/4) then K is given, as before, by:

$$K = -M/(1-M^2) \pm \Delta \text{ (upper sign for } \underline{x} > 0 \text{ and lower sign for } \underline{x} < 0) \tag{14}$$

Again, the actual root is then found by Muller's method (reference 3).

Having determined the root for a plug flow at M_{av} with $dp/d\underline{y} = 0$ at $\underline{y} = 0$ (symmetric case) and $p = 0$ at $\underline{y} = 0$ (antisymmetric case), the root for a parallel sheared flow at $M(\underline{y})$ can be determined by analytic continuation as follows. Let $dM(\underline{y}) = M(\underline{y}) - M_{av}$, where M_{av} is the average Mach number across the duct. Then consider a sequence of parallel sheared flow problems at $M_i(\underline{y})$ where :

$$M_i(y) = M_{av} + s\,(dM(\underline{y})) \tag{15}$$

and s is varied in steps of 0.01 from 0 to 1. At s = 0, we have the plug flow at M_{av} and at s = 1, we have a parallel sheared flow at $M(\underline{y})$. For each s, the eigenvalue problem is solved by Muller's method (reference 3), where the procedure is to (a) start with known boundary conditions at $\underline{y} = 0$, (b) integrate the differential equation pair for F

and F_1 and (c) determine (for the chosen K) how well the boundary condition at $\underline{y} = 2$ is satisfied. At s = 1, the solution of the full problem is complete.

Concerning the integration of the differential equation pair for F and F_1', a very simple predictor-corrector method is used to go from known values of F and F_1 at $\underline{y}$ to $\underline{y}+d\underline{y}$. In the first step, F and F_1 are advanced to $\underline{y}+d\underline{y}$ based on the known values at $\underline{y}$. Call these values F^p and $F_1{}^p$. In the next step, F and F_1 are advanced using the mean of the (known) values at $\underline{y}$ and the initial "prediction" at $\underline{y}+d\underline{y}$, namely F^p and $F_1{}^p$. The user is asked to provide some guidance on the nature of the variation of $M(\underline{y})$ from $\underline{y} = 0$ to $\underline{y} = 2$. Two parameters y_l and y_u are requested such that $0 \le \underline{y} \le y_l$ delineates a boundary layer region near the $\underline{y} = 0$ wall and $y_u \le \underline{y} \le 2$ denotes the region near the $\underline{y} = 2$ wall. The Mach number $M(\underline{y})$ may vary rapidly due to blowing and the boundary layer near $\underline{y} = 2$. These regions and the region $y_l \le \underline{y} \le y_u$ are subdivided into 1000 intervals of equal width for purposes of integration of the differential equation pair by the predictor-corrector method. In the future, a more sophisticated method of integration of the differential equation pair may be adopted.

This method has been tested in terms of its ability to reproduce the results in figures 5 and 7 of reference 2 for (in the notation of reference 2) $M_c = 0.36$ and $\omega = 5$. This was done for selected displacement thicknesses, for the case of a "turbulent" boundary layer profile (designated as (T) in reference 2). Good agreement is obtained on the calculated attenuation rates between the present study and reference 2.

3. Use of CFD to Design and Evaluate Blowing Schemes for Flow Profile Alteration

A. Design of Blowing Scheme

An analytical assessment was performed with the use of CFD and the modal duct propagation tool discussed in Section 2 to better understand the effects of near-wall flow profile alteration on the absorption of a forward propagating sound wave by an acoustic liner. The results of this study provided guidance in the determination of the optimum combination of flow profile and liner impedance for maximum noise attenuation, and led to the development of a blowing device that was designed to alter the near-wall Mach number profiles in a 51 mm by 51 mm duct. CFD was used to characterize the effects of various geometric and flow injection parameters on resulting Mach number profile alteration, and identify the optimal injection configurations for achieving the greatest increase in liner attenuation by blowing.

CFD calculations were based on a 51 mm channel with a free stream centerline Mach number of approximately 0.45 (corresponding to approximate experimental flow conditions). The effects of injection angle and injection slot height were investigated. Injection angles ranging from 10° to 60° and slot heights ranging from 2.5 mm to 3.8 mm were considered, while injection mass flow was held at 10% of the main duct flow. The corresponding injection Mach number ratio and momentum ratio were also investigated. A commercially available CFD code (CFX 5.6®) was used to perform the 2nd order accurate, steady state calculations. The Shear Stress Transport (SST) turbulence model was employed with automatic near-wall treatment. A structured, multi-block grid was generated for each calculation with a minimum of 15 nodes in the boundary layer at all locations. A simple two-dimensional channel was considered with injection located 130 mm downstream of the inlet. This provided a developed boundary thickness of approximately 4 mm at the point of injection. The total channel length was set at 640 mm to allow full mixing of the injected jet prior to the channel exit plane. Differences in surface roughness due to a soft wall liner were not accounted for in the simulations.

Each CFD solution was analyzed at 6 discrete equally-spaced axial planes, beginning 25 mm downstream of the point of injection and spanning a 150 mm axial length, representing the length of wall treatment considered in actual testing. Mach number profiles were extracted at each plane and interrogated for parameters defining the blowing layer, such as Mach number overshoot, blowing wall displacement thickness, blowing stream width, and centerline Mach number. Mach number overshoot, f_M, is defined in Eq. 16 where M_{max} refers to the peak local Mach number in the wall jet.

$$f_M = \frac{M_{\max}}{M_c} - 1 \tag{16}$$

A schematic of the injection plenum is shown in Figure 2. The plenum was designed with a slot to plenum area ratio of approximately 40 to achieve proper flow stagnation within the chamber. The transition from plenum to injection slot was created with a smooth, circular arc, ending tangent to the channel upper wall, thus creating a Coanda effect on the flow exiting the slot. This provided a uniform injection stream and prevented separation of the wall jet at the slot exit. The throat of the slot was positioned at the plane normal to the exit of the lower slot lip, allowing the flow to accelerate along the full length of the slot arc.

CFD predicted Mach number contours with injection at angles of 10°, 30° and 60° and slot height 3.8 mm, corresponding to a Mach number ratio of 1.4, are shown in Figure 3. Injection at 60° resulted in severe boundary layer separation, leading to a large recirculation region downstream of the slot exit and subsequent high losses. Injection at 30° did not result in separation, however was found to provide small penetration into the free stream as the jet is bent toward the wall at the point of injection, leading to an initial high acceleration along the inner radius of the jet curvature and locally excessively high (sonic) Mach numbers and high losses. Shallow injection angles on the order of 10° to 20° were found to be optimum, allowing jet profiles to fully develop without excessive loss. Injection at 10° supported Mach number ratios as high as 2.0, corresponding to a slot height of 2.5 mm for 10% mass injection. Predicted Mach number profiles with this configuration are shown in Figure 4. These profiles initially exhibit a thin blowing layer with high peak Mach number overshoot, and then gradually decay to a wider blowing layer with moderate Mach number overshoot (~50% of injection Mach number overshoot 150 mm downstream) as the jet momentum mixes with the free stream.

Recall that the intended result of injection is to alter the near wall flow gradient by creating a peak Mach number, and thus a reduced or negative displacement thickness along the region of acoustic liner surface. With this in mind, the average displacement thickness and Mach number overshoot due to blowing over a 150 mm length have been plotted in Figure 5 as functions of injection angle at an injection Mach number ratio of 1.4 (slot height 3.8 mm). A trend of decreasing displacement thickness with decreasing injection angle is shown, while a similar trend of increasing Mach number overshoot with decreasing injection angle is apparent. These results support the above conclusion of shallow injection angles providing better wall jet development with minimized loss.

B. Integration of CFD Predictions and Acoustic Code

Results of the CFD analysis were integrated into the duct propagation code. As the code allows for arbitrary Mach number profiles, acoustic attenuation for the individual profiles extracted from CFD calculations can be predicted for a desired frequency and impedance set. As noted in Section 3A, CFD results were analyzed at six discrete axial locations, equally spaced 25 mm apart, along the 150 mm length associated with an acoustic liner. To calculate the associated attenuation for each profile, the Mach number profiles were individually input to the duct propagation code along with the desired acoustic frequency and liner impedance values. The output of the code was the amount of attenuation provided by the liner over a 25 mm length. To determine the total attenuation across the 150 mm liner, the attenuations per 25 mm associated with each of the six profiles were summed. In general, little variation for each respective injection condition in attenuation per 25 mm length was predicted along the 150 mm length of liner. This finding agrees with the fact that the injection wall displacement thickness showed only a slight increase along the length of liner, again supporting the suggested dependency of attenuation on displacement thickness. Note that the duct propagation predictions assume an infinitely lined duct and therefore do not account for liner leading or trailing edge reflections. Also, all acoustic predictions are for the lowest order mode only. As a result, only acoustic frequencies up to 3 kHz were investigated.

Four impedance sets were considered in these predictions. The first of these corresponded to a Ceramic Tubular Liner (CTL) previously tested at NASA Langley. The normalized impedance profile for this liner at a centerline Mach number of 0.5 is provided in Table 1. Three other "virtual" liners were also considered. (Note that all prescribed impedances assume sound oscillations as $\exp(i\omega t)$). These liners are characterized by a frequency-independent normalized resistance of 2.00 and normalized reactance of $(2\Omega/28.15 - \cot(\Omega\iota/h))$ with honeycomb depths of ι=3.4 mm, 6.9 mm and 10.3 mm. Here $\Omega=\omega h/c$ with $\omega = 2\pi f$ (f is the sound frequency in Hz), h= half duct width =25.4 mm, and c is the speed of sound assumed to be 341 m/s. These impedance sets (designated as I2, I3 and I4) have frequency-dependent reactance as detailed in Table 1. The predicted baseline attenuation resulting from the no-blowing Mach number profiles predicted with CFD for each impedance set over a 150 mm length are provided in Figure 6.

Attenuation calculations were made for all blowing configurations studied, encompassing injection angles ranging from 10° to 60° and slot heights of 2.5 mm and 3.8 mm, with corresponding range of Mach number ratios from 1.4 to 2.0. Shown in Figure 7a is the predicted improved attenuation achieved by blowing for each injection configuration, based on the CTL impedance set. Improved attenuation is defined here as the difference in predicted attenuation across a 150 mm length of liner with and without blowing. Predicted changes in attenuation based on the CFD predicted blowing profiles show the CTL impedance set to be relatively insensitive to the various injection configurations. Changes in attenuation consistently range from $\pm$2dB, with reductions in attenuation due to blowing at higher frequencies. Shown in Figure 7b is a similar comparison based on the I3 impedance set. Here, a significantly different trend in improved attenuation is found, as attenuation consistently increases with frequency. Clear distinction in the influence of injection configuration is also evident in this plot, as the shallow injection angles with higher injection Mach number ratio show the greatest levels of improvement over baseline attenuation.

Shown in Figure 8 is a comparison of improved attenuation due to blowing across all four impedance sets for an injection configuration of 10° and slot height 2.5 mm. Impedance sets I2 and I3 appear to be the most responsive to blowing, with trends of increasing attenuation improvement with increasing frequency, while I4 appears responsive only at the lower end of the frequency spectrum, similar to the CTL impedance set. These trends were found to repeat with all remaining blowing configurations.

Recall that the blowing configuration of 10° injection and slot height of 2.5 mm, corresponding to a Mach number ratio 2.0, achieved the greatest reduction in displacement thickness and the highest Mach number overshoot, as averaged across the 150 mm length of liner. Figure 9 demonstrates the relationships between improved attenuation and Mach number overshoot and displacement thickness for all predicted injection configurations with the I3 impedance set. At lower frequencies, the improved attenuation appears somewhat flat as Mach number overshoot increases, however this dependence increases dramatically as frequency increases. This result agrees with the findings of Nayfeh (reference 2) that refractive effects become more prominent with increasing acoustic frequency. A similar trend is found in the plot of improved attenuation versus displacement thickness, where improved attenuation levels increase as the injection wall displacement thickness is reduced. These results point to the blowing configuration of 10° injection and slot height 2.5 mm as a prime candidate for further investigation, as this configuration achieved the greatest reduction in displacement thickness with the highest Mach number overshoot, and thus the greatest improvement in attenuation. An additional 30 dB of attenuation was predicted with this blowing configuration at 3 kHz with the I3 impedance set. Note on the plot of improved attenuation versus displacement thickness in Figure 9 that the curves of improved attenuation cross the zero axis and turn negative at a point corresponding to the baseline, no-blowing displacement thickness of 0.5 mm. This further implies that reduction in displacement thickness is a driving parameter toward improved attenuation of the lowest order acoustic mode, whereas an increase in displacement thickness diminishes the attenuation.

As a result of this analysis, two acoustic liners were chosen for further testing. These included the CTL (150 mm length) and a NASA Langley designed/fabricated liner corresponding to the impedance set I3 (150 mm length). The CTL, while shown to be fairly insensitive to near-wall flow profile alteration, was chosen for testing because it is a thoroughly studied and well-understood liner. This liner will be useful for validation of attenuation models and better understanding the dependence of attenuation improvements due to blowing on impedance characteristics. Conversely, a new liner based on impedance set I3 was chosen due to its predicted high responsiveness to wall injection. This combination of liners is expected to provide increased understanding of the influence of liner impedance on the effectiveness of inlet wall injection on liner attenuation.

C. Sensitivity of Predicted Attenuation Improvements Due to Blowing

A study was performed to assess the sensitivity of attenuation improvements with blowing to variations in the resistance and reactance of impedance set I3. The blowing configuration of 10° injection and slot height 2.5 mm, corresponding to a Mach number ratio 2.0 was considered, with the results shown in Figure 10. By varying the normalized resistance of I3 by a nominal $\pm$0.5, little sensitivity was observed at the lower end of the frequency spectrum. However, at higher frequencies this variation was amplified, with a difference in predicted improved attenuation of up to 10 dB. Similar results for lower frequencies were found when varying the normalized reactance by a nominal $\pm$0.5; however, at higher frequencies the attenuations only appear sensitive to an increase in reactance. These results indicate that while increased improvements in attenuation are possible with higher frequencies, the sensitivity to the actual impedance characteristics realized by a liner is also increased. This result provides a certain level of understanding of the importance of liner design and the ability to realize exact impedance values on expected results due to blowing.

An additional study was performed to assess the sensitivity of attenuation improvements with blowing relative to the baseline, no-blowing flow profile. For this study, three baseline flow profiles, referred to as P1, P2 and P3, were altered, with identical blowing schemes of 10° injection angle and 10% mass injection through a 2.5 mm slot. As shown in Figure 11a, the first two profiles considered (P1 and P2) have well developed cores and vary in boundary layer thickness by a factor of approximately two. The third profile, P3, based on a measured inlet profile in the NASA Langley GIT, has a considerably different profile with no true core and boundary layers covering approximately 90% of the duct span. The goal of this study was to assess the predicted improvement in attenuation of the lowest order mode due to blowing in the presence of these three widely varying baseline flow profiles.

Predictions of the baseline acoustic attenuation with impedance sets I1 (CTL) and I3 are shown in Figure 11b. It is apparent for the I3 impedance set that baseline attenuation is highly dependent on the initial flow profile, with maximum variations between profiles greater than 50%. However, the CTL impedance set does not show a great dependence on the initial flow profile, agreeing with earlier conclusions that this impedance set is insensitive to variations in flow profile. Figure 11c shows the improved attenuation due to blowing for each profile. Here it is seen that the variations in improved attenuation around the mean values of the three profiles are significantly less than

those of the baseline attenuation. It is suggested that this similarity is due to comparable levels of profile alteration achieved relative to the individual baselines with identical blowing schemes. The average reduction in displacement thickness due to blowing across the length of liner for the three profiles is ~3.6 mm, with only 10% variation between profiles.

4. EXPERIMENTAL METHODS AND RESULTS (NASA LANGLEY GRAZING INCIDENCE TUBE)

A. Test Section Description

Experimental evaluation of the effects of inlet blowing on the absorption properties of two acoustic liners was conducted with the NASA Langley Grazing Incidence Tube (GIT), which contains an 812 mm-long test section (figure 12) with internal dimensions of 51 mm x 51 mm. A high-pressure air source and a pair of vacuum pumps were located, respectively, upstream and downstream of the test section. This combination was used to achieve a desired mean flow Mach number (flow is from left to right) under near-ambient conditions. For the current study, the centerline Mach number (measured approximately 75 mm downstream of the test section trailing edge) was set to 0.4. Discrete frequency sound was injected 0.4 m downstream of the test section using a sinusoidal signal supplied by a function generator to two BMS 4590 compression drivers. The acoustic waves emitted from the acoustic drivers simulated an inlet condition (sound propagation from right to left) across the surface of the 150 mm-long test liner, and into the plenum section upstream of the test section. The surface of the liner formed the upper wall of that portion of the test section. Elsewhere, the test section sidewalls were rigid.

Tests were conducted with and without a flow injection (blowing) device, which was mounted upstream of the acoustic liner location. Service air was supplied to the blowing device to achieve an injection mass flow rate of 49 g/s. At each test frequency, the sound pressure level (SPL) at the upstream plane (as measured by a reference microphone) was set to 120 dB. This setting was chosen to balance the need to limit the sound pressure levels to the linear regime with the need to maximize the signal-to-noise ratio for the full test sequence.

B. Test Liner Configurations

Two acoustic liners (see figure 13) were used in the current study. The first was a single-layer ceramic tubular liner, and the second was a two-layer wire-mesh liner. The ceramic tubular material was chosen because its resistance is dominated by internal fluid viscosity and is thus very insensitive to mean flow effects. As a result, the effects of air injection on the impedance of this liner were not expected to be significant. Thus, for the ceramic tubular liner, any improvements in the attenuation as a result of air injection were expected to be a direct result of improved refractive effects. The two-layer liner facesheet was constructed with a wire-mesh material. It was therefore expected to be more nonlinear than the ceramic tubular liner. This liner was designed to achieve similar impedance characteristics to that of impedance set I3 in Table 1 for the frequency range of 1.5 to 2.5 kHz, as this impedance set was predicted to be highly responsive to modified boundary layers. Measurements have not yet been made to assess the actual impedance characteristics achieved by this liner in the presence of grazing flow. The two liners, shown schematically in figure 13, are described in detail here:

(a) As depicted in figure 13-a, the ceramic tubular liner consisted of "sinusoid-shaped" parallel channels embedded in a ceramic matrix. These channels, with equivalent circular diameters of 0.76 mm, were perpendicular to the exposed surface and provided a surface porosity of 65%. The 88.9 mm-deep channels were rigidly terminated such that each was isolated from its neighbor to ensure a locally reacting structure. The structure of this liner results in an impedance spectrum that is linear with respect to acoustic pressure, insensitive to grazing flow, and is a reasonably good absorber over the frequency bandwidth used with the GIT. Previous studies conducted at NASA Langley Research Center have demonstrated that the acoustic characteristics of this type of liner enabled it to serve as a "calibration liner" for validating impedance eduction schemes in the GIT (see reference 5). Consequently, it was chosen as a baseline for the current investigation.

(b) As depicted in figure 13-b, the two-layer liner contained two wire-mesh screens, each with a DC flow resistance of 580 MKS Rayls. The depths of each of the two layers were 3.2 mm, and their nonlinearity factor (as quoted by the manufacturer) was 1.3. The deviation from a nonlinearity factor (NLF) of unity is an indicator that this liner should be expected to be sensitive to changes in acoustic pressure and/or grazing flow. However, with a NLF of 1.3, this sensitivity was low enough that modifications of the boundary layer profile were expected to have a more significant effect on refraction than on the impedance of the liner.

C. Acoustic Measurement Procedure

Acoustic tests with and without blowing were conducted for each of the two acoustic liners, such that blowing effects could be assessed. The test section (see figure 12), which contained 95 flush-mounted 6.35 mm-diameter microphones, was designed to educe liner impedances in high speed grazing flow and high SPL. In order to assess the attenuation of the test liners, data acquired with the 32 microphones mounted on the lower wall were required. The data at each of these microphone locations was stored such that future comparisons with 2-D acoustic propagation predictions would be possible.

For the current investigation, discrete tones (one at a time) were injected downstream of the test section. Tests were conducted at source frequencies of 0.5 to 3.0 kHz, in steps of 0.5 kHz, with the mean flow Mach number set to a centerline value of 0.4. This frequency range was chosen such that the broadband acoustic performance of each liner could be determined with only the lowest order hard-wall mode cut on in the duct. This restriction is consistent with the usage of 2-D analysis. For each data acquisition, 2000 averages on each microphone channel (blocks of 2048 data points per average) were used. To reduce the influence of flow noise, a cross-spectrum signal extraction method (see reference 4) was used to determine the amplitudes and phases at each of the microphone locations.

D. Mean Flow Profile Procedure and Results

A traversing Kiel probe and a wall-mounted static pressure port were used to acquire mean flow profiles (liner replaced with a hard-wall section) approximately 40 mm and 290 mm downstream of the blowing device, such that the change in flow profile over the length of the liner could be assessed. Five traverses were conducted in each section, 3 horizontal (12.7, 25.4 and 38.1 mm above lower duct wall) and 2 vertical (12.7 and 38.1 mm from side duct wall). Flow profiles measured at the upstream plane for the two selected test conditions (injection mass flow rates of zero and 49 g/s, with centerline Mach number of 0.4) are provided in figure 14. As shown in this figure, the effects of the blowing device were significant up to 5 mm from the upper wall. At the downstream location (figure 15), the effects of blowing diffuse outward to about 20 mm from the upper wall.

E. Acoustic Results

As described earlier, acoustic measurements were conducted for both liners at air injection mass flow rates of zero and 49 g/s. The results provided in figure 16 show SPL profiles acquired for the ceramic tubular liner with and without blowing, at frequencies of 0.5 and 2.0 kHz. Figure 17 provides the corresponding results achieved with the wire-mesh liner. As is clearly evident from these figures, the ceramic tubular liner provides significantly more absorption than the wire-mesh liner for the case of no blowing. Although all of the frequencies are not included (for the sake of brevity), the presented results are typical of those acquired at most of the test frequencies. For the majority of the test frequencies, the SPL decay (from downstream to upstream end of the liner) is observed to be fairly linear over the length of the ceramic tubular liner, both with and without blowing. A similar linear trend is observed for the wire-mesh liner at 2 kHz when blowing is introduced. Without blowing, however, the SPL profile for this liner is dominated by a standing wave pattern at 0.5 kHz, and thus the corresponding attenuation is minimal. Table 2 contains a listing of the estimated attenuations achieved in the NASA Langley GIT for each of the two liners, both with and without air injection. These attenuations were estimated by comparing the SPL at the trailing edge of the liner (nearest the acoustic source) with the corresponding SPL at the leading edge of the liner. For the cases with linear decay, the accuracy of the estimates is $\pm$0.5 dB. For the cases where a standing wave pattern was dominant, the general trend of the data was used to estimate the attenuation. The estimated attenuation for these SPL profiles has an increased uncertainty (estimate depends upon amplitude of standing wave) of at least $\pm$1 dB. This was considered acceptable, since those cases where the attenuation was obscured by the standing wave pattern offer sufficiently low attenuation to be of minimal interest.

As shown in figure 18, a blowing rate of 49 g/s has no observable effect on the attenuation (that can be resolved using the current test procedure) for the ceramic tubular liner. This is in agreement with trends established during initial predictions. For the wire-mesh liner, however, the effects of air injection are evident. At the higher frequencies (2.0 to 3.0 kHz), the attenuation achieved with this liner is noticeably increased. In fact, the increase in attenuation due to air injection at 3.0 kHz is 10 dB. However, it should be noted that the amount of attenuation is a function of the duct geometry. As stated before, the impedance spectra of the ceramic tubular liner is known to be very insensitive to mean flow (see reference 5). Therefore, air injection should have minimal effect on the impedance of this liner, and only refractive effects would be expected to be relevant. On the other hand, since the wire-mesh liner is slightly nonlinear (NLF of 1.3 for wire-mesh facesheet), it is more responsive to flow injection (i.e., impedance sensitivity to flow). In light of this, there are two possible explanations for the increase in attenuation for this liner with air injection. One possibility is that alteration of the boundary layer profile modifies the acoustic impedance such that a more optimal value (for the GIT) is achieved. The second is that changing the refraction angle (redirecting sound toward the walls) is responsible for the increased attenuation. Additional tests are

needed to confirm either of these possible explanations, but this initial evidence suggests that boundary layer profile modification offers potential for improved inlet noise attenuation.

5. Summary

A collaborative investigation has been conducted at General Electric Global Research Center and NASA Langley Research Center to investigate the effects of boundary layer profile modifications on the absorption of acoustic liners. A duct mode propagation analysis was developed to predict the optimum combination of liner impedance and boundary layer profile to achieve maximum absorption in the NASA Langley Research Center Grazing Incidence Tube (GIT). This analysis incorporates the refractive effects of the modified boundary layer profile.

In order to determine realistically achievable boundary layer profiles, a parametric study was conducted using Computational Fluid Dynamics (CFD) analysis. This CFD analysis was used to determine the optimum design for a blowing device to be incorporated into the GIT to achieve the boundary layer profile predicted (using the modal analysis) to provide maximum increased attenuation. This combination of modal analysis (for acoustics) and CFD (for mean flow) also accounted for the gradual change of the boundary layer profile over the length of a liner to be tested in the GIT.

Finally, an experimental evaluation was conducted in the NASA Langley GIT using a blowing device (air injector) designed using the process described above. Two liners were evaluated with and without blowing (air injection mass flow rates of zero and 49 g/s). The first was a ceramic tubular liner, which was known to be linear (insensitive to changes in acoustic pressure and mean flow). This liner was used as a baseline for comparison purposes. The second was a two-layer wire-mesh liner, which was slightly more nonlinear (nonlinearity factor of the wire mesh was 1.3). This liner was designed to provide the optimum impedance that corresponded to the boundary layer profile achieved with a blowing rate of 49 g/s.

The attenuation of the lowest order acoustic mode achieved with the ceramic tubular liner was observed to be virtually insensitive to this amount of blowing, whereas an increase in attenuation of up to 10 dB was measured for the wire-mesh liner. Clearly, the results are duct-geometry dependent, but this offers encouragement for continued investigation of the usage of boundary layer profile control for enhanced acoustic attenuation. Two possible explanations for the increase in attenuation with the wire-mesh liner should be considered for this continued investigation. The first is that alteration of the boundary layer profile modifies the acoustic impedance such that a more optimal value (for the GIT) is achieved. The second is that changing the refraction angle (redirecting sound toward the walls) is indeed responsible for the increased attenuation. Future investigations will be conducted to more thoroughly evaluate these two possibilities.

References

1. Unruh, J.F. and Eversman, W., "The Utility of the Galerkin Method for the Acoustic Transmission in an Attenuating Duct," J. Sound & Vib., 23(2), 187-197 (1972).
2. Nayfeh, et al, "Effect of Mean Velocity Profile Shapes on Sound Transmission Through Two Dimensional Ducts," J. Sound & Vib., 34 (3), 413-423 (1974).
3. Press, et al, "Numerical Recipes", p.364, Second Edition (1992).
4. Bendat, J.S. and Piersol, A.G., "Random Data: Analysis and Measurement Procedures,"Wiley-Interscience, 1971.
5. Jones, M.G., Watson, W.R., Parrott, T.L., Smith, C.D., "Design and Evaluation of Modifications to the NASA Langley Flow Impedance Tube," AIAA 2004-2837, 10th AIAA/CEAS Aeroacoustics Conference, Manchester, England, 2004.

Figures and Tables

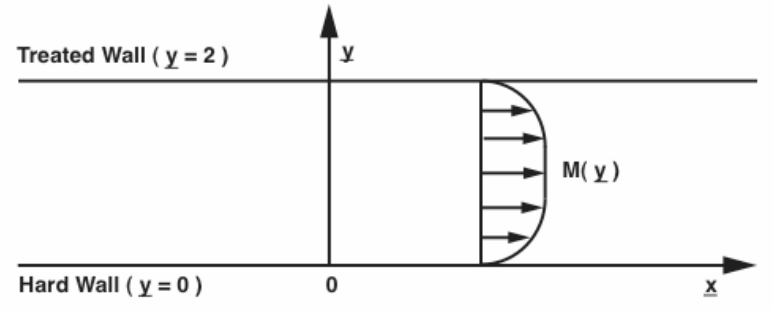

Figure 1. Sketch of coordinate system used in acoustic analysis.

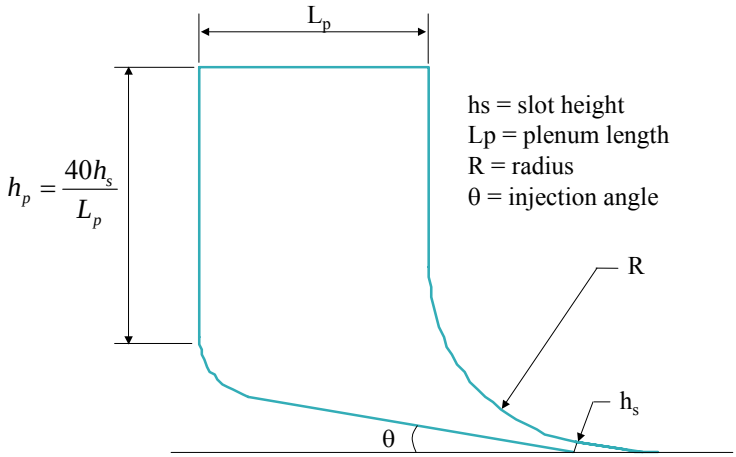

Figure 2. Schematic of injection plenum.

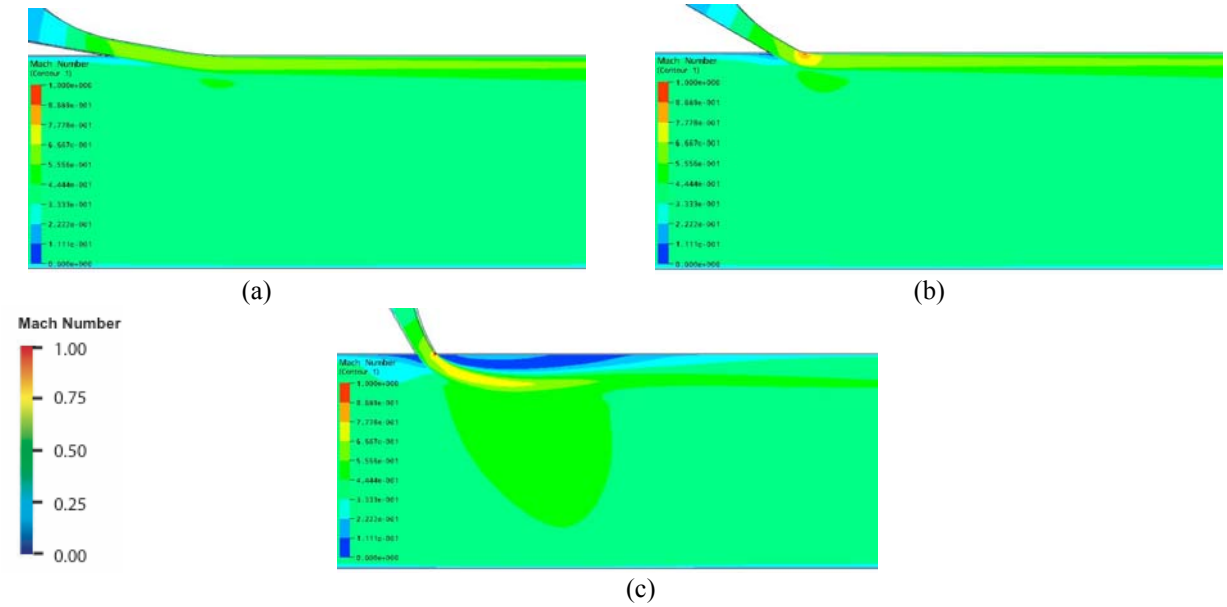

Figure 3. CFD Mach number contours of 10% mass injection and slot height 3.8 mm for injection angles of (a) 10°, (b) 30° and (c) 60°.

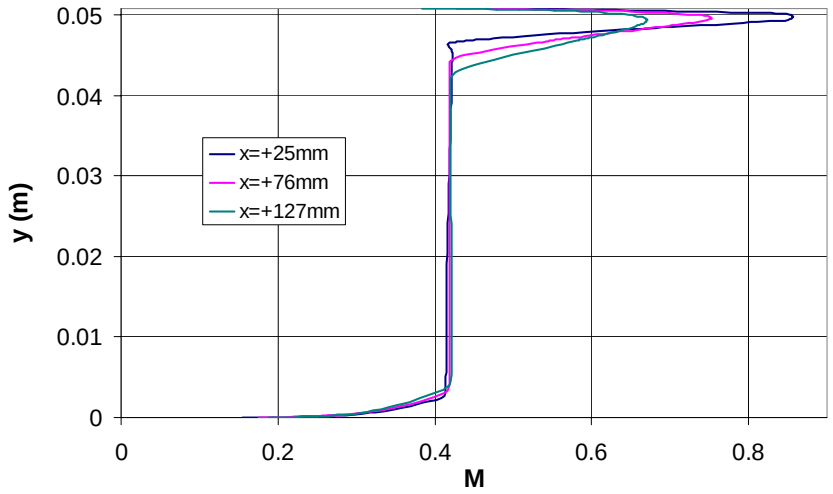

Figure 4. CFD predicted Mach number profiles with 10% mass injection through a 2.5 mm slot at 10° (injection at x=0).

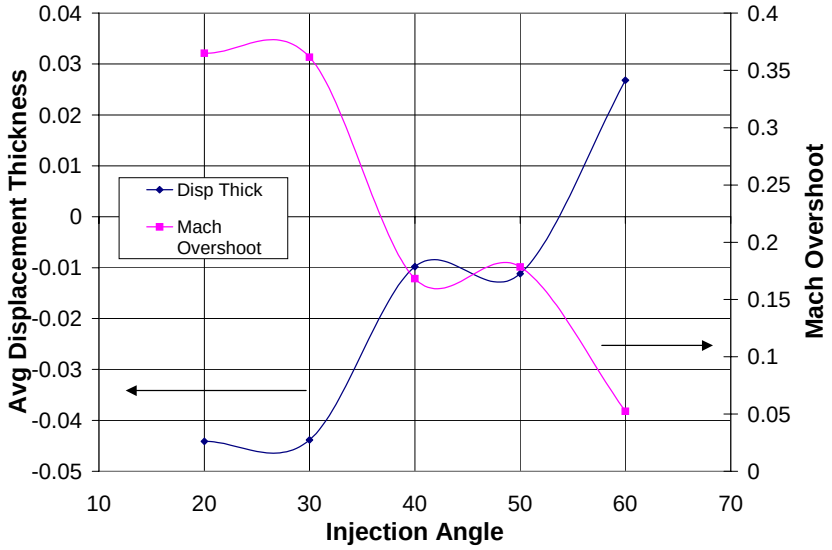

Figure 5. Average displacement thickness and Mach number overshoot over 150 mm length downstream of 10% mass injection as functions of injection angle.

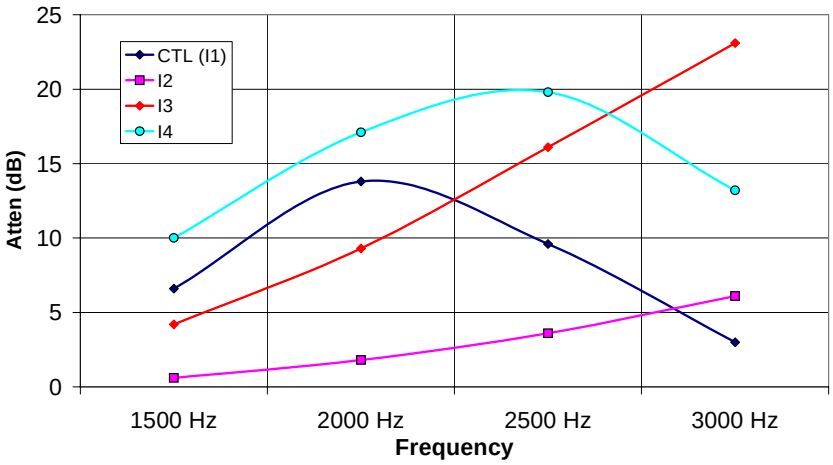

Figure 6. Predicted baseline, no blowing attenuation of four impedance sets considered based on parametric CFD analysis (lowest order acoustic mode).

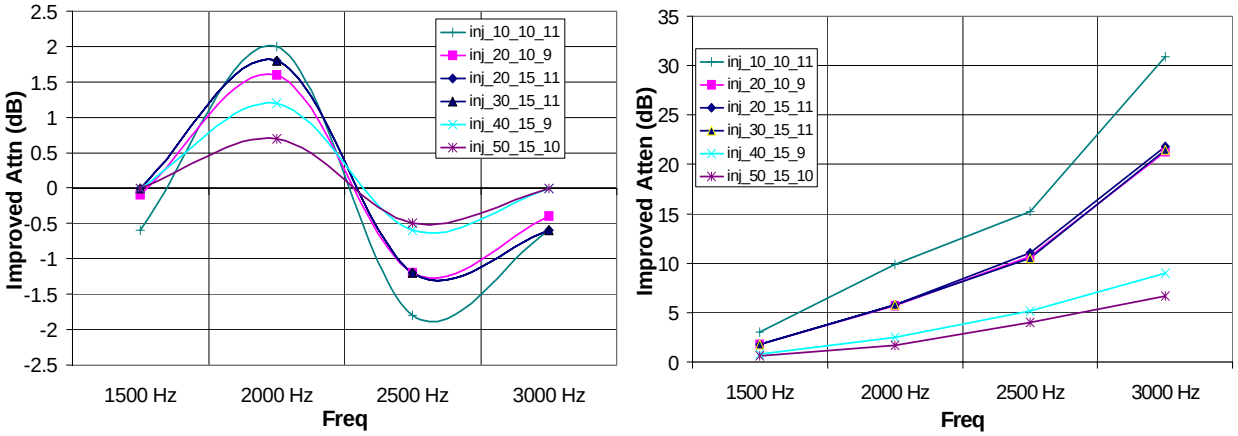

(a) (b)

Figure 7. Predicted improved attenuation for CFD predicted injection configurations with the a) CTL impedance set and b) I3 impedance set (lowest order acoustic mode). Legend represents injection angle, slot height, and injection mass ratio.

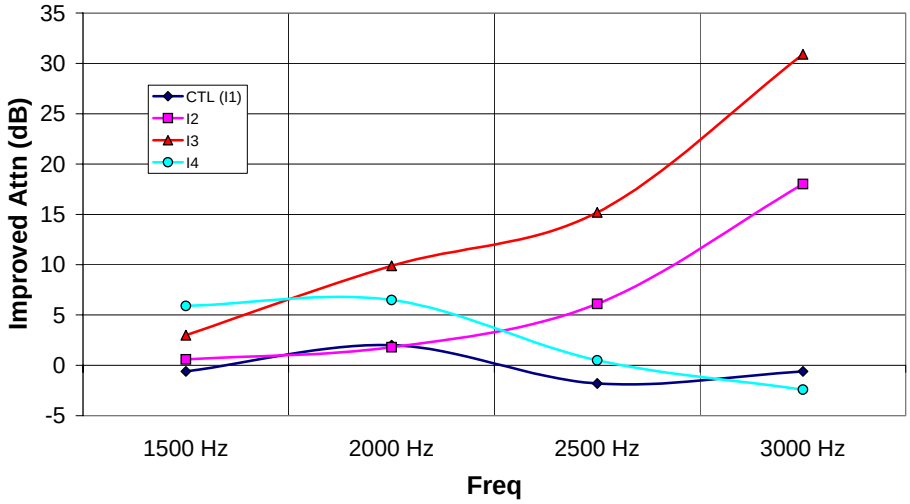

Figure 8. Predicted improved attenuation based on CFD prediction of injection at 10°, slot height 2.5 mm and 10% mass for each of the four impedance sets considered (lowest order acoustic mode).

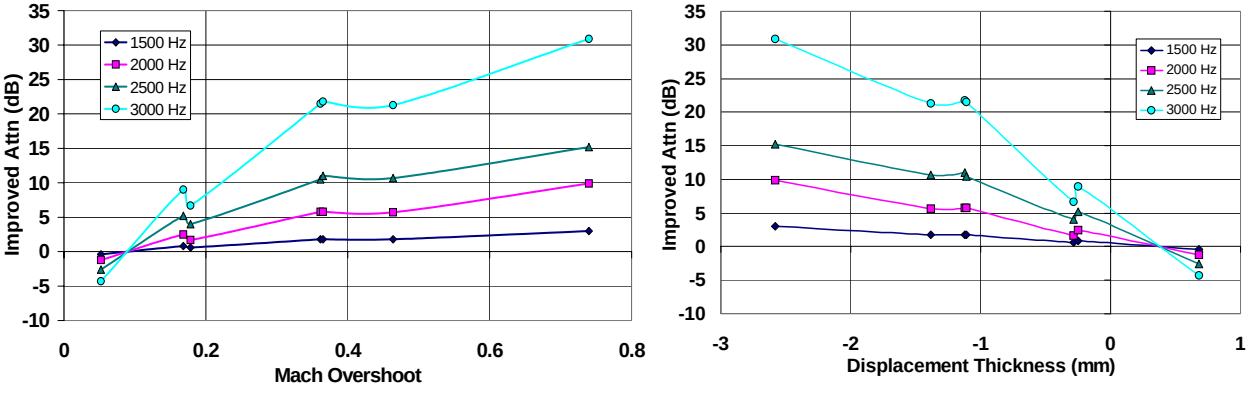

(a) (b)

Figure 9. Predicted improved attenuation for CFD parametric injection configurations plotted in terms of (a) local Mach number overshoot and (b) local displacement thickness (lowest order acoustic mode).

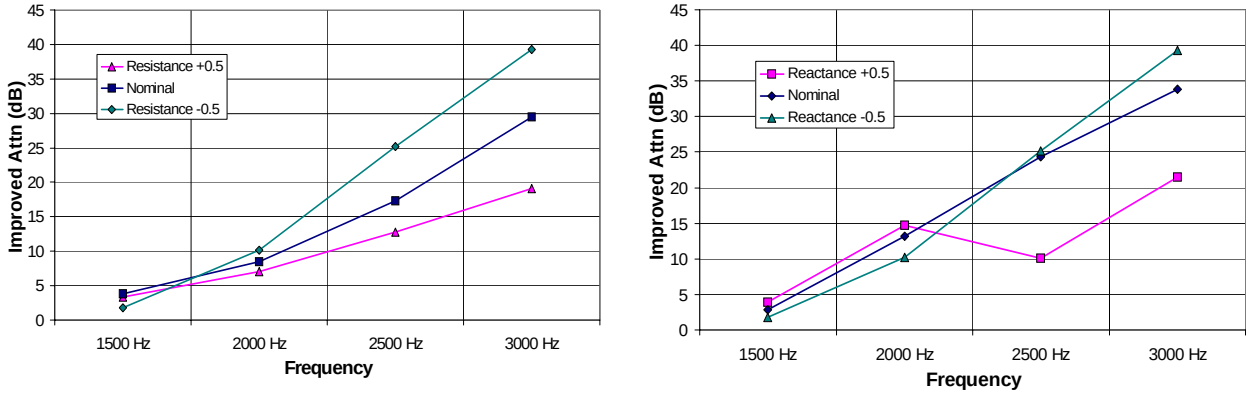

(a) (b)

Figure 10. Sensitivity of predicted attenuation improvements for the 10°, Mach number ratio 2.0 injection configuration to variations in impedance set I3, a) resistance b) reactance (lowest order acoustic mode).

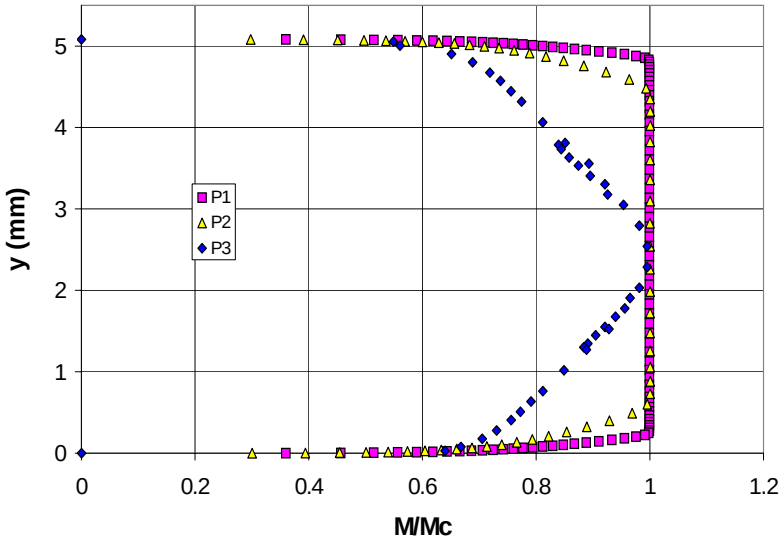

(a)

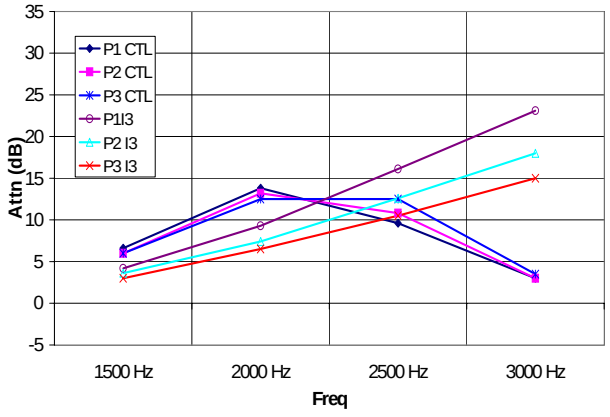

(b)

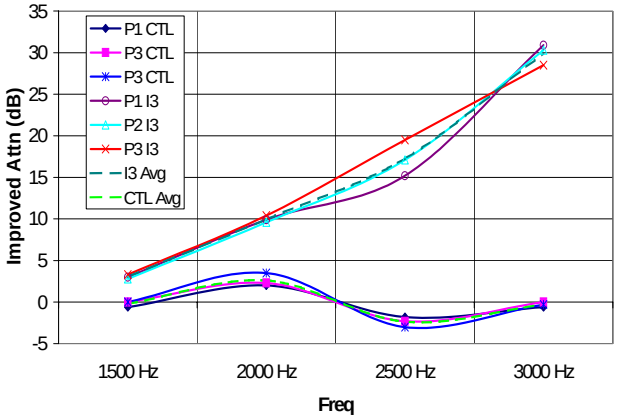

(c)

Figure 11. (a) Baseline flow profiles considered in sensitivity study of attenuation improvements due to blowing. (b) Predicted baseline attenuation for the I1 (CTL) and I3 impedance sets of the three flow profiles considered in sensitivity study (lowest order acoustic mode). (c) Predicted improved attenuation for the I1 (CTL) and I3 impedance sets of the three flow profiles considered in sensitivity study (lowest order acoustic mode).

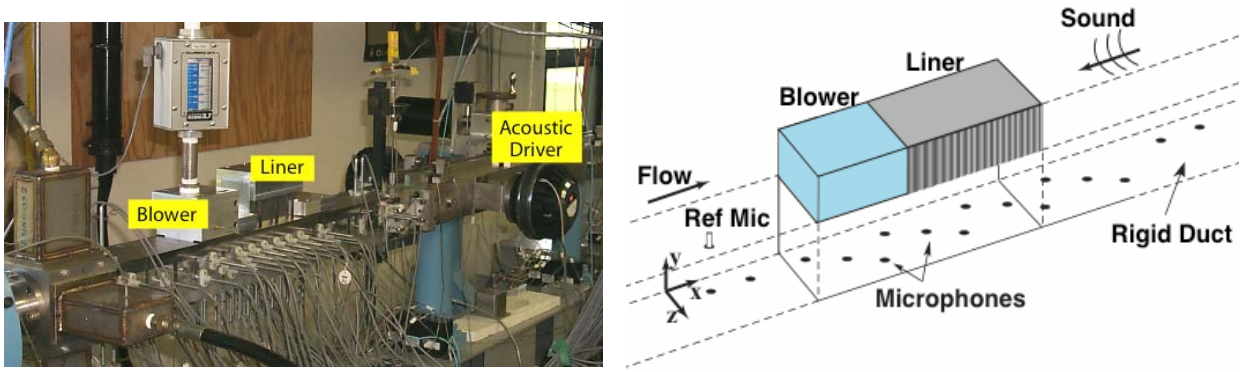

Figure 12. Photograph and sketch of NASA Langley Research Center Grazing Incidence Tube Test Section.

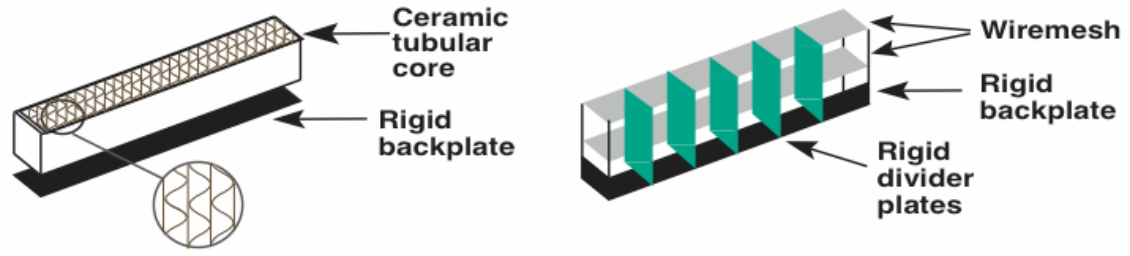

Figure 13. Sketch of ceramic tubular and two-layer wire-mesh liners.

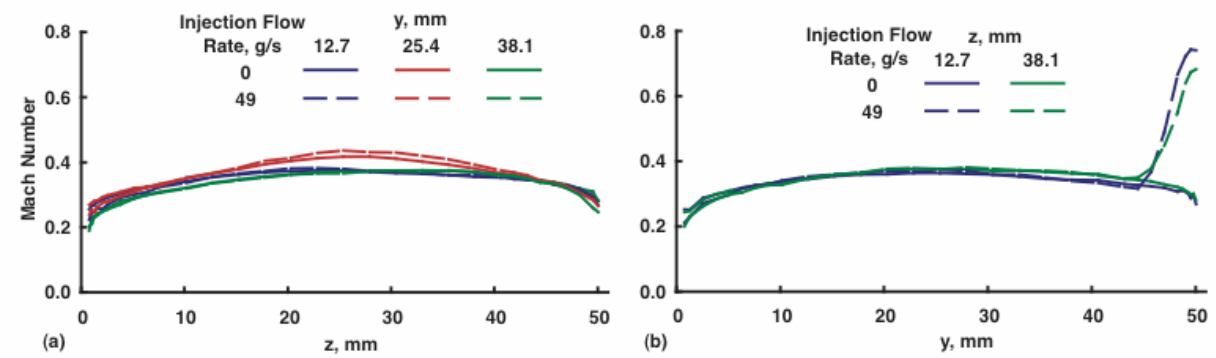

Figure 14. Upstream flow profiles at air injection mass flows of zero and 49 g/s – (a) horizontal, (b) vertical.

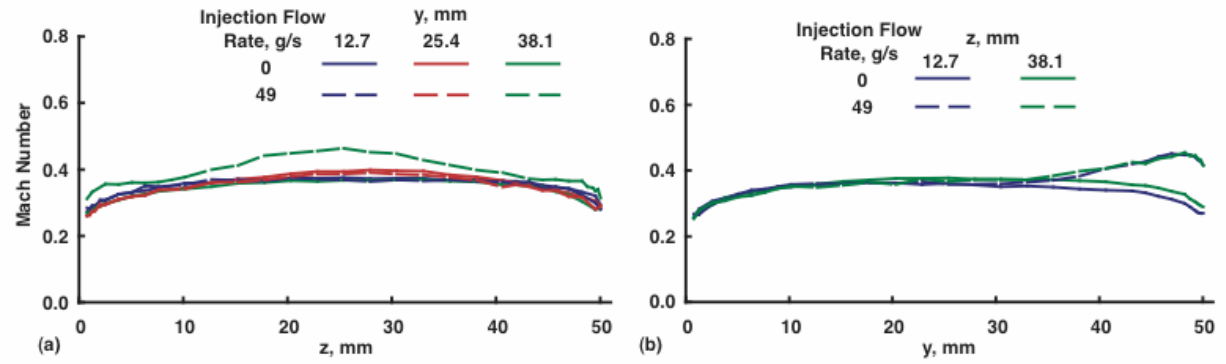

Figure 15. Downstream flow profiles at air injection mass flows of zero and 49 g/s – (a) horizontal, (b) vertical.

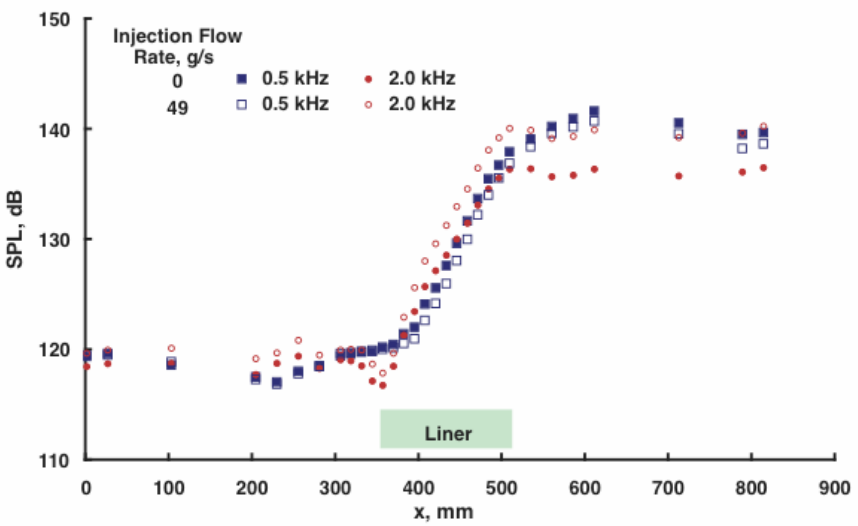

Figure 16. SPL profiles for ceramic tubular liner at 0.5 and 2.0 kHz, with and without blowing.

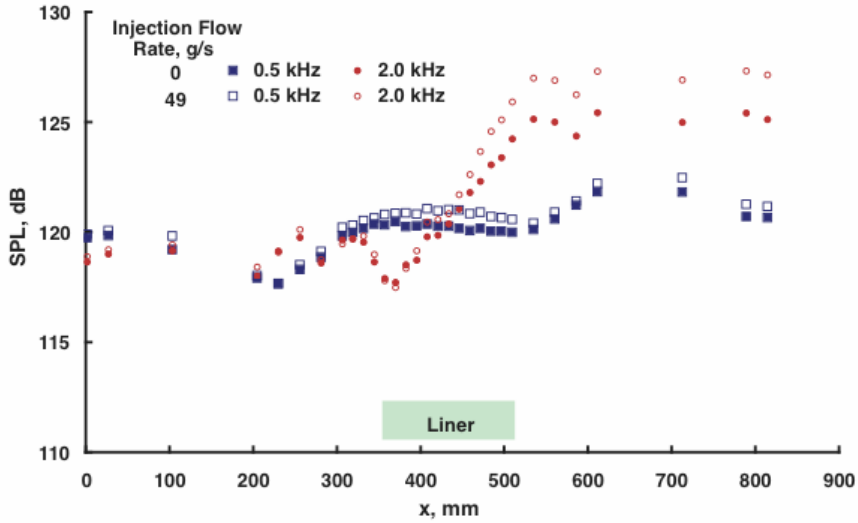

Figure 17. SPL profiles for wire-mesh liner at 0.5 and 2.0 kHz, with and without blowing.

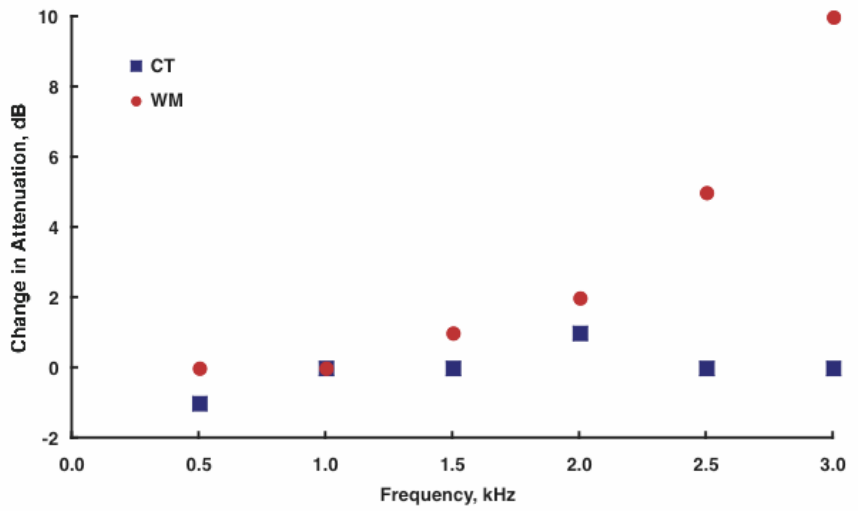

Figure 18. Effects of blowing on attenuation (attenuation with blowing minus attenuation without blowing) for ceramic tubular (CT) and wire-mesh (WM) liners.

Table 1. Normalized impedances of acoustic liners considered in analysis (constant normalized resistance of 2.00 for impedance sets I2, I3 and I4).

Frequency (kHz)	I1, CTL Resistance	I1, CTL Reactance	I2, ι=3.43 mm Reactance	I3, ι=6.86 mm Reactance	I4, ι=10.29 mm Reactance
1.5	1.40	1.24	-10.47	-5.16	-3.37
2.0	2.53	-1.24	-7.80	-3.81	-2.44
2.5	1.09	-0.75	-6.19	-2.98	-1.87
3.0	0.77	-0.06	-5.11	-2.41	-1.46

Table 2. Estimated attenuations achieved with each liner, with and without blowing.

Frequency (kHz)	Ceramic Tubular Liner		Wire-Mesh Liner	
	Attenuation, dB (0 g/s)	Attenuation, dB (49 g/s)	Attenuation, dB (0 g/s)	Attenuation, dB (49 g/s)
0.5	18	17	0	0
1.0	16	16	2	2
1.5	9	9	4	5
2.0	20	21	6	8
2.5	9	9	10	15
3.0	5	5	12	22